Proceedings World Geothermal Congress 2026
Calgary, Canada, June 8 – 11, 2026

Stratigraphy, Alteration Mineralogy, Permeability and Temperature Conditions of Well OW-710C, Olkaria North-East Field, Kenya.

Koilege Timothy[1], Helga Margret Helgadottir[2] and Hjalti Franzson[2]
[1]Kenya Electricity Generating Company Plc, 785 Naivasha, Kenya
[2]Iceland GeoSurvey Urdarhvarfi 8, 203 Kópavogur, Iceland
tkoilege@kengen.co.ke

Keywords: Hydrothermal alteration, Permeability, Olkaria, Lithology, Temperature.

ABSTRACT

Well, OW-710C, is a directional well drilled in the Northeast Olkaria geothermal field to a depth of 3136 m from cellar top (CT). Drilling and analysis revealed the following lithological units; pyroclastics, rhyolite, basalt, intermediate rock, trachyte, tuff, breccia and intrusions. Hydrothermal alteration shows evidence of water-rock interaction, fluid pathways, chemical and physical conditions of the system, whose products occur as replacement and/or precipitation in vesicles and veins. Prograde alteration is evident in the well with low temperature alteration minerals encountered at shallow depth and progressively increasing with depth. There is, however, evidence of retrogression at depth where calcite is overprinting epidote thus indicating probable cooling condition. Five alteration zones were established with first appearance of temperature dependent minerals. Below the unaltered zone, fine-grained clays- zeolites are found succeeded by course-grained clays, epidote, and actinolite-epidote zones. Evidence of small and medium feed zones are postulated below the production casing. However, mineralization especially with calcite may have sealed the once permeable feed zones. Intersection of the Ololbutot fault zone at 1174 m CT may have caused an overall increase in permeability, however, it may have contributed to the relative cooling due to influx of cooler fluids. The reservoir temperature measurements appear to be stable between 1200-1450 m CT of around 256°C but then gradually lower to 215°C at 3100 m CT after 29 months of heat recovery.

1 INTRODUCTION

Geothermal exploration and development in Olkaria geothermal complex started in the 1950's with two exploratory wells drilled in 1956 and the second, X2 drilled to a depth of 1035 m giving good results of 235°C (Clarke, et al., 1990). However, focus was shifted to a detailed surface exploration of Eburru, Olkaria and Bogoria geothermal fields later in 1970 and from the review in 1972, Olkaria prospect was given a priority. Since then, stepwise drilling and development began with the 15 MWe Olkaria 1 power plant constructed in 1981. The current installed capacity in the geothermal area is 950 MWe run by KenGen and independent producers in Olkaria west (Orpower Ltd.) and Oserian development company to the northwest. Olkaria Northeast field has approximately 70 drilled wells with some connected to the 105 MWe Olkaria II power plant.

Well, OW-710C is a directional well drilled in the Olkaria Northeast field, a sub-sector of the Greater Olkaria Volcanic Complex (GOVC). It is approximately 1.2 km west of Olkaria II power station and defined by UTM coordinates zone 37N, 9904553.612m northing and 198156.3486 m easting and at an elevation of 2059.849 m.a.s.l as shown in figure 1. This well was drilled with the aim of catering additional steam for Olkaria I unit IV and V and at the same time appraise the extent of the resource northwest of well OW-710. Drilling commenced on 30th July 2014 and was completed 28th September 2014 under the 80 wells contract. It was drilled to a depth of 3136 m CT with surface, anchor, and production casings set at 45.5, 397 and 939.5 m CT, respectively.

This study aims to establish the reason for the general decrease in permeability down the well despite the interception of the Ololbutot fault zone at mid-trajectory. Furthermore, the study will define the alteration zones, the current and historical thermal conditions of the geothermal system and location of permeable zones in the well. Lastly, an understanding of the rock and mineral chemistry, crystallization patterns, sequence of mineral formation and precise composition of minerals within the rock matrix.

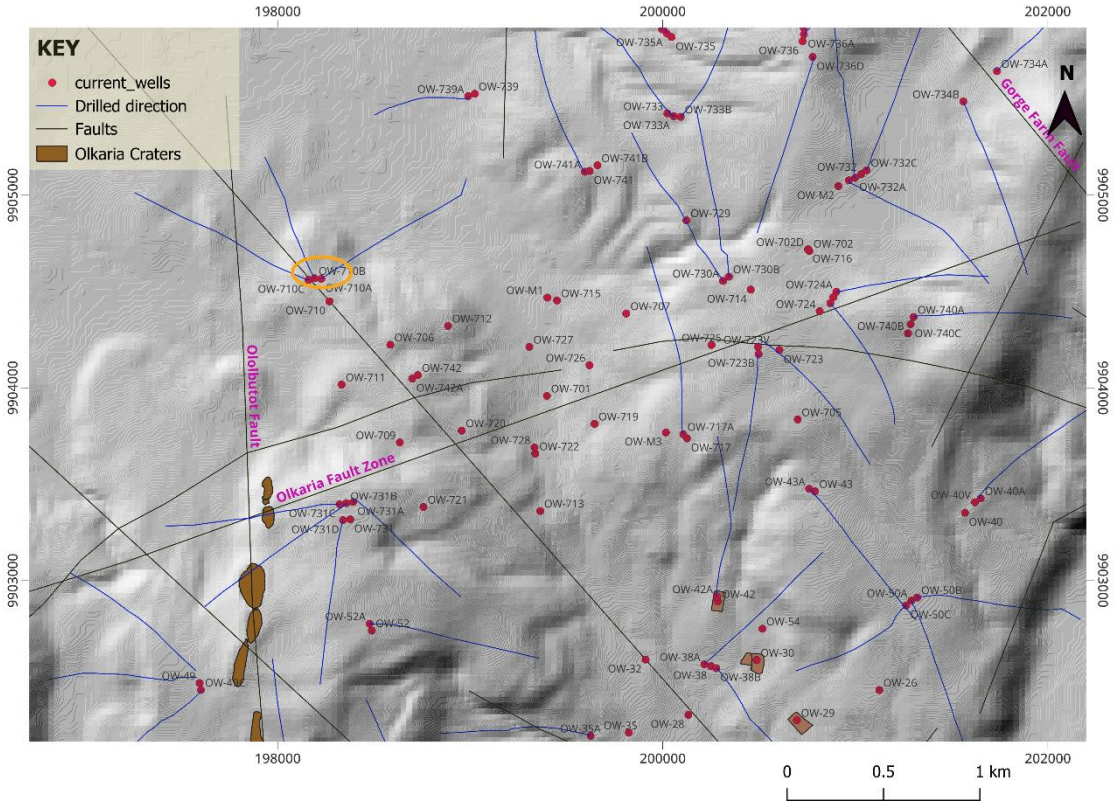


Figure 1: Location of well OW-710C (circled in yellow)

2 GEOLOGY AND STRUCTURAL SETTING

2.1 Regional geology

The East African Rift System (EARS) is an intra-continental ridge system with a series of half-grabens or troughs (basins/rift valleys) bordered by uplifted shoulders and filled with volcanic rocks and/or sediments. The eastern part of the EARS runs from the Afar region in Ethiopia in the north through the Turkana depression, the Kenya rift valley to the North-Tanzania divergence in the south shown in figure 2 (Conti, et, al., 2021, Chorowicz., 2005). The Kenya rift valley can be categorized into the northern, central and Nyanza rifts with Lake Bogoria area located almost at the centre of the Kenyan dome forming a triple junction. The northern part comprises two parallel valleys running from lake Turkana half graben southwards to the area around Lake Baringo. It is separated by the Kamasia block, an uplifted faulted block lying between Elgeyo escarpment and Lake Bogoria (Chapman, 1978). The Nyanza rift extends westwards and disappears into Lake Victoria. The central rift is marked by a sharp bend immediately after lake Bogoria. It is bounded by high rift shoulders, the Mau escarpment to the west and the Aberdare escarpment to the east rising about 3000 m and 4000 m, respectively. The rift floor elevations of about 2000 m steadily descend southwards to about 600 in Lake Natron (Strecker, 1990, Chorowicz, 2005).

Volcanic activity in the rift started in the Miocene period with extensive phonolite and basalt eruptions in the uplifted dome and formation of a half-graben. Rock outcrops of these eruptions are observed in Uasin Gishu and Yatta plateaus, overlying the late Proterozoic gneisses and schists of the Mozambique belt. It later transitioned to basalt and trachyte eruptions. In the late Miocene, grid faulting commenced accompanied by large pyroclastic eruptions and basalt/trachyte volcanism succeeded by full graben formation and development of major faults. Later in the early Pleistocene, fissure eruptions of trachyte and basalt occurred proceeded by deepening of the axial zone of the rift and extensional tectonics in the narrow zones. Afterwards eruptions and rifting led to the formation of late Quaternary to recent volcanoes with extrusion of rhyolites, basalts, phonolites and pyroclastics. These volcanoes are associated with geothermal activity in the rift (Omenda, 1998, Clarke, et al., 1990) and include Olkaria, Eburru, Longonot, and Suswa.

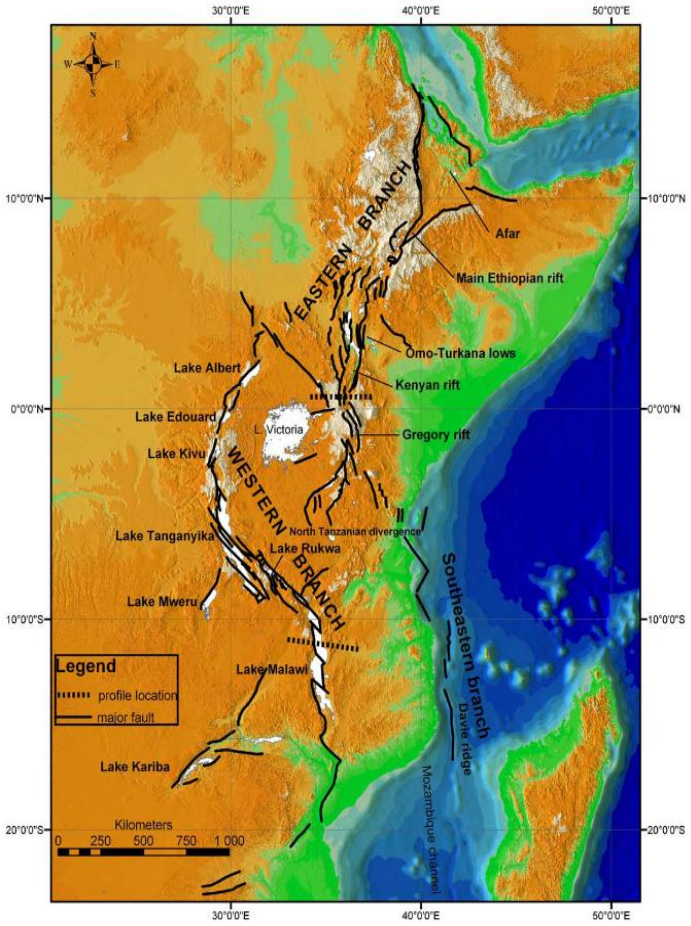


Figure 2: Hypsographic DEM of the East African Rift System showing the location of the eastern and western branches (Chorowicz, 2005).

2.2 Geology and structural setting of the Olkaria geothermal field

Olkaria geothermal complex is a multicentred volcanic field bounded by Eburru, Longonot and Suswa to the northwest, east and south. It is about 240 km^2 and is commonly termed complex because it does not form a distinct volcanic centre but comprises approximately 80 volcanic centres. The centres are characterised by steep sided domes and thick lava flows of restricted lateral extent. Olkaria hill, standing about 340 m high with a basal diameter of approximately 2 km, is the most prominent dome which is used as a reference point in naming of wells. To the east of the hill is the Ololbutot ridge with a fissure system comprising series of narrow and deep craters responsible for a recent lava eruption ~ 180 BP with very blocky rock outcrops (Clarke, et al., 1990).

The surface geology in Olkaria mainly comprises comenditic rhyolites, pumice falls and volcanic ash deposits and volcaniclastic deposits near lake Naivasha as shown in figure 3. Most pyroclastic fall deposits are from Longonot volcano to the west and some as far as Suswa volcano to the south. Data analysis by Omenda (1994, 1998) from rock cuttings and cores from drilled wells revealed four distinct lithostratigraphic groups in the subsurface. The upper Olkaria volcanics that comprised comendite flows, pyroclastics, trachytes and minor basalt. These are succeeded by the Olkaria basalt that overlie the plateau trachytes and consists of mainly basaltic flows, with minor intercalations of trachytes, tuffs and minor rhyolites. These basalts are common in the eastern side of Olkaria hill but lacking in Olkaria west field. The plateau trachytes mainly comprise trachytes and minor layers of rhyolites, basalts and tuff. It is the main reservoir rock east of Olkaria hill. Lastly, are the Mau tuffs that are prevalent in Olkaria west consisting mainly of tuffs, with minor interlayers of trachytes, basalts, and rhyolites. There exists a major discontinuity influenced by the N-S trend through Olkaria hill that cause absence of the Mau tuffs beyond the hill.

Structures provide important channels for fluid flow in a geothermal system. However, sometimes they form barriers that restrict or divert flow. The occurrence and distribution of geothermal manifestations such as intense fumarolic activities, altered grounds and hot or warm grounds are fracture controlled. Prominent faults in the Olkaria geothermal system include the Olkaria fault zone, ENE-WSW structure that runs from north of

Olkaria hill, intersecting several faults to Gorge-farm fault to the east. The young N-S Ololbutot fracture and fault, responsible for recent volcanism in the area with intense fumarolic activities and altered grounds, are observed on the surface especially around Hobleys volcano located east of well OW49 and south of well OW731 (Omenda, 1998). To the NE of the study well and at the boundary of Olkaria Northeast field, is the Gorge-farm fault, striking NW-SE. The fault is marked by an aligned group of hills/domes extending about 8 km northwards and 5 km wide and is responsible for recharging the geothermal system. Temperature models for the field have shown low temperature measurements recorded in wells around the Gorge farm (Okoo, et, al., 2017, Koilege, 2018). Further eastward between Olkaria east and Domes field is the, the Ol Njorowa gorge, a prominent erosional feature that extend about 16 km in a NE-SW direction. It is an active fault zone evidenced by extensive fumarolic activities along it and occurrence of numerous dykes and volcanic plugs (Otieno, et, al., 2014). Lastly is the proposed ring structure marked by alignment of arcuate rhyolitic domes and steep sided ridges in the field believed to indicate the presence of a buried caldera. However, the hypothesis has not yet been proven owing to the presence of thick pyroclastic fall deposits extending to about 300 m depth as observed in the drilled wells obscuring any surface structures, especially in the Olkaria Domes field (Omenda, 1998).

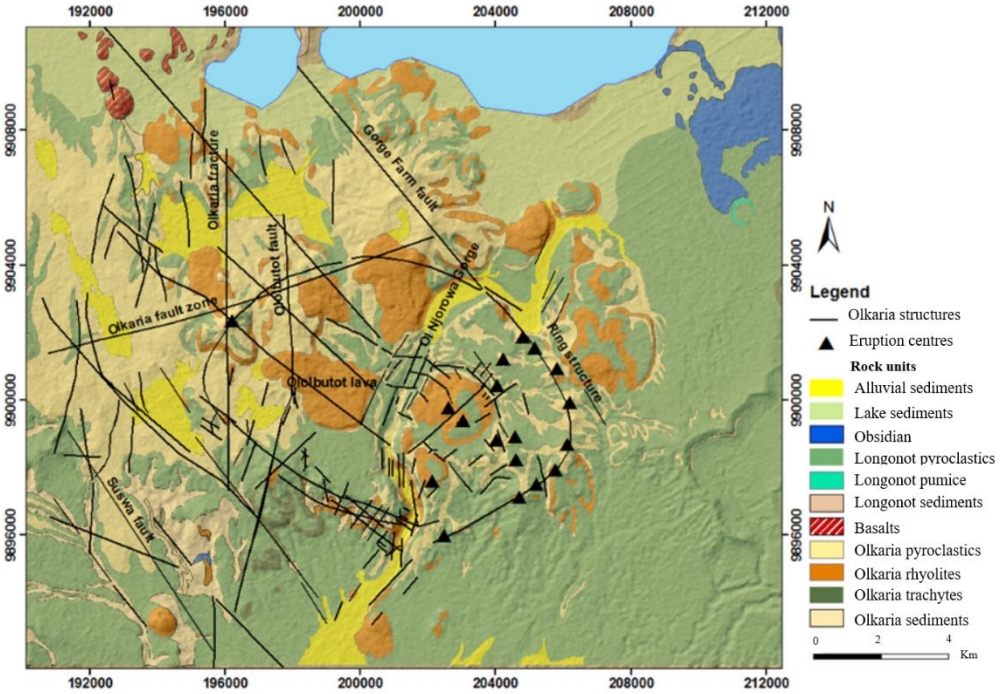


Figure 3: Map showing structures and surface geology of Olkaria geothermal field (Modified by Munyiri, 2016 from Clarke, et al., 1990).

3 RESULTS: BOREHOLE GEOLOGY

3.1 Stratigraphy of well OW-710C

The general lithostratigraphic units encountered in this well are analogous to other already drilled wells in the Olkaria geothermal complex. Based on studies (Omenda, 1998, Lagat, et.al. 2005) and comparison to borehole geology data from already drilled wells, four main formations lithostratigraphic units were observed. Upper Olkaria volcanics that form the uppermost unit from surface to 740 m CT; underlain by the Olkaria basalts from 740 to 940 m CT. The following succession is the plateau trachyte from 940 m CT and extends all the way to well bottom. The last group of rocks are the Olkaria intrusive rocks that form thin layers within the plateau trachyte succession. The characterization of rock samples provides useful information on the nature and type of the geothermal system and origin of rocks (Wohletz, et.al. 1992). Analysis revealed the following units as described below and presented in figure 4.

3.1.1 Olkaria volcanic products

Pyroclastics: This is the uppermost rock unit in the well between 0 t0 26 m CT, and comprises unconsolidated mixed fragments of pumice, volcanic glass, tuffs, and rhyolite. It is moderately oxidized but with no hydrothermal alteration.

Rhyolite: This is the dominant rock unit in the upper Olkaria volcanics but also occurs as thin layers in the basalt and trachyte formations at depth. They appear white, grey to brown, fine-grained, porphyritic with distinct quartz and feldspars phenocryst and minor mafic minerals. It is fractured and with minor vesicles infilled with secondary minerals. The rock is relatively massive and exhibits minor alteration intensity. However, in the fractured zones it moderately to highly oxidized. The unit was encountered between 56m and 740 m CT.

Tuff: Occurrence of tuff marks different eruption episodes in the area as well as zones of enhanced permeability. It formed thin interbeds ranging between 14 and 38 m thick. Two types of tuffs were encountered in the well and described depending on the texture, grain size and composition.

Rhyolitic tuffs: These are the common varieties of tuff observed in this zone between 128-190, 336-360, 542-560, 598-628 m CT. Generally, they appear as vario-coloured from brown, grey to pale green, fine to cryptocrystalline rock composed of silicic minerals that have been embedded within the fine volcanic ash flows. Lithic rock fragments and quartz crystals cemented in ash matrix are observed at 336-360 m and at 542-560 m, where the rock appears welded with thin wavy streaks in the rock matrix. The formation often appears vesicular and some zones between 542-560 and 598-628 m CT are fractured and exhibit slight to moderate alteration intensity. Oxidation is mainly confined to the shallower depths down to 360 m CT.

3.1.2 Olkaria basalts

Basalts were first encountered at 560 m in the upper zone, but a thick succession that forms the main lithofacies was encountered between 740-822 m although its lower boundary could not be defined due to major loss of circulation at 822-940 m CT. It is the main unit capping the geothermal reservoir as well as a marker horizon stratum used to delineate fault displacement in the geothermal field. The rock is dark grey to brown, fine-grained, porphyritic composed of plagioclase feldspar phenocrysts and ferromagnesian minerals. It shows slight to moderate alteration and its vesicles and microfractures are infilled with calcite, quartz, and chlorite.

3.1.3 Plateau trachytes

The succession mainly comprises trachytes with minor intercalations or thin layers of rhyolite, basalt, intermediate rock, breccias, tuffs, and intrusions. It is the most dominant rock in the well and forms the reservoir rock of the Olkaria geothermal system. At shallower depth, the rock appears aphyric but at depth from 1200 m CT it is phyric with distinct crystals observed in the groundmass. The unit has a wide range of colours with the less altered appearing white to light grey whilst the altered counterpart is mostly pale-green-dull grey to brown. It is fine grained, often porphyritic with prismatic sanidine and quartz phenocrysts and sporadic mafic minerals. Evidence of lava flow is observed in some fragments with distinct flow structure and elongated feldspar crystals showing a preferred orientation.

Breccia: This is a rare rock that form zones of enhanced permeability. The Earth Science Australia compiled notes between 1995-2021 on energy and minerals, which gives a precise classification of breccias based on the amounts of rock clasts, veins, clasts matrix and chemically deposited cement within the breccia. This was used to classify the breccias encountered into two types, i.e., fault breccia and magmatic intrusive breccia and is described as follows;

Fault breccia: It was encountered between 1162 and 1174 m CT and formed due to the grinding action of two fault planes and emplacement of broken rock fragments. It appears brown to pale-grey, tuffaceous rock with angular and sub-angular clasts composed of feldspars, glassy crystals, lithics embedded in fine matrix. The rock is highly fractured and brecciated with notable veinlets infilled with clays. Some fragments appear vesicular with minor infills of clays and secondary quartz. The formation shows moderate alteration intensity.

Magmatic intrusive breccia: The unit was encountered at depth from 1764 to 1792 m CT. It may have been formed during magma emplacement of the intrusive micro-granite lying below it at 1792-1820 m CT for it contains broken clasts of trachyte, fresh mafic minerals, feldspars, and glassy fragments cemented in fine matrix. It appears earth brown and slightly fractured and brecciated with minor veinlets. It shows moderate alteration but extensive oxidation which may be attributed to contact metamorphism.

Intermediate rock: This is a fine-grained crystalline rock unit observed at depths from 1566-1586 m and 1742-1764 m CT. It is grey, felsic rich, porphyritic rock with tiny quartz crystals, indistinct feldspars, and rare mafic minerals. The formation appears slightly fractured but is relatively fresh with minimal alteration intensity observed.

Trachytic tuff: This is the main tuff unit below 1000 m CT and occurs as thin layers within the trachytes. The rock is observed between 1440-1454, 1974-2002, 2020-2058, 2092-2116, and 2300-2326 m CT and appears brown, grey to greenish, heterogeneous, and furthermore rich with feldspar crystals as well as lithics and glassy fragments compacted in fine tuffaceous matrix. The tuff appears fractured and vesicular with infills of secondary quartz, green clays, calcite, and epidote

3.1.4 Olkaria intrusives

Minor Olkaria intrusives were encountered in this well occurring as thin, discrete units ranging from 4 to 28 m thick. Intrusions facilitate heat transfer into the geothermal system and are originated from a deeper magma source. Furthermore, they may enhance permeability where zones around the observed units showed slight to intense fracturing evidenced by increased vein fillings and minor losses of circulation. Three types of intrusives were encountered in this well; micro-granite, micro-gabbro, and basaltic dyke.

Micro-granite: This is the main intrusive type observed in the well and it appeared white-light grey, fine to medium grained porphyritic rock with distinct quartz and feldspar phenocrysts and specs of mafic minerals. The rock is massive and dense and was observed at 1792-1820, 2122-2130, 2634-2650, 2790-2796, and 3068-3078 m CT.

Micro-gabbro: It is also referred to as dolerite and appeared as dark-grey, holocrystalline mafic rich rock with plagioclases and ferromagnesium minerals. It was encountered between 2772-2784 m CT.

Basaltic dyke: The unit was observed between 2714-2718 m. It is dark-grey fine grained, porphyritic rock with distinct plagioclases and mafic minerals. It is relatively fresh with no observable hydrothermal alteration.

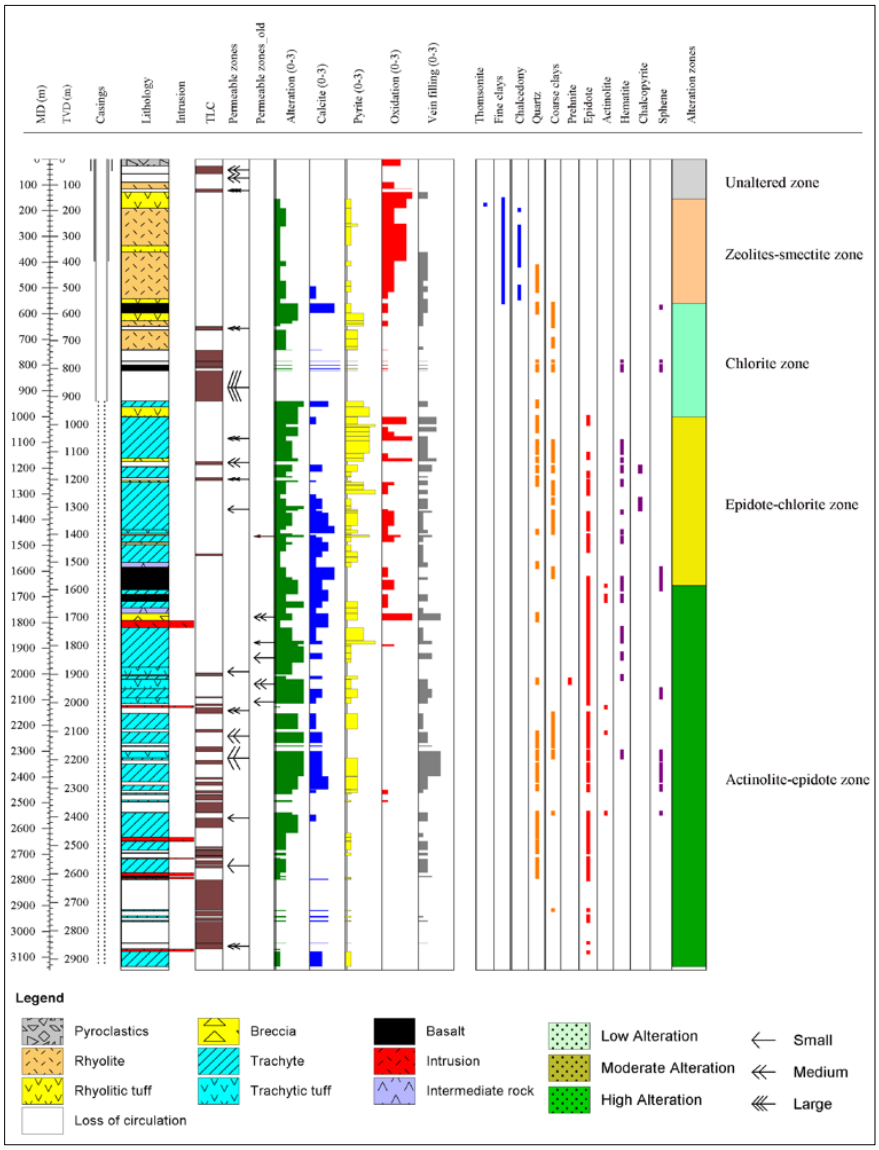


Figure 4: Lithology, alteration mineralogy of well OW-710C

3.2 Hydrothermal alteration mineralogy

Hydrothermal alteration is a process in which primary minerals, such as feldspar, pyroxene, and olivine, are replaced by secondary minerals often under specific temperature conditions. This process is evident in the mineral chemistry and physical appearance of the rock as well as texture and structure of minerals (Shanks III, 2010). Composition of the host rock, permeability, fluid chemistry, temperature and pressure conditions and duration of fluid-rock interactions influence their occurrence and distribution (Browne, 1984). This is because hydrothermal alteration gives a direct evidence of water-rock interaction, fluid pathways and chemical and physical conditions of the minerals precipitated.

3.2.1 Distribution of hydrothermal alteration minerals, depositional sequence, and alteration zones

The occurrence and distribution of hydrothermal alteration minerals was used to map alteration zones, permeability indicator minerals and depositional sequence. The low temperature alteration minerals including fine-grained clays, zeolites, chalcedony, and quartz, are observed in the uppermost part of the well at 0-560 m CT. However, quartz mineralization and oxidation persist down the well. This oxidation may imply the incursion of cooler groundwater at some stage in history in the upper part of the geothermal system. Oxidation can also be a part of the contact alteration around solidifying intrusions at depth. An example to this may be at the margin of the intrusion below 1700 m. Below this, we have the occurrence of coarse-grained clays (chlorite), quartz, hematite and sphene between 560-1000 m CT and they signify zones of moderate temperatures. Lastly, at depth high temperature alteration minerals are persistent especially epidote in association with sphene, actinolite, and prehnite occurring sporadically. Other minerals observed at depth include quartz, hematite, chlorite and chalcopyrite. The mineral distribution is presented in figure 4.

Permeability networks was also qualitatively analysed to characterize zones of enhanced water rock interactions. The minerals, pyrite, secondary quartz, calcite, and oxides, were observed throughout the well whilst platy calcite was encountered sporadically at 784-822, 1424-1440, 1586-1634, and 1690-1718 m CT. Their concentration and form together with fracture density in rocks were used to determine zones of enhanced and restricted permeability. Earlier studies by Browne (1970) showed that feldspar alteration is the most sensitive mineral at higher temperature and permeability, thus zones with high alteration were also incorporated to define the permeability networks in this well. Apart from indicator minerals, losses of circulation and temperature logs were also used.

The analysis of mineral depositional sequences, binocular microscope, and scanning Electron microscopy (SEM) was used to characterize the cross-cutting relationship of alteration minerals in veins, vesicles, and within the rock matrix. This is the where the younger mineral occur in the innermost part whilst the older in the outermost part. The sequence gives a clue on the changes of a geothermal system over time (Gebrehiwot, 2010, Kandie, 2017).

Mineral paragenesis, in well OW-710C, were analysed and broadly categorized three different sections: the upper, middle and the lower zones. Within the upper zone between 0-560 m CT, analyses showed that low to medium temperature alteration minerals infillings are prevalent. Below this, the middle section shows infill of medium temperature alteration minerals comprised of secondary quartz, chlorite, and minor calcite. The lower zone below 1800 m CT, epidote is the dominant mineral in veins and vesicles with minor secondary quartz, chlorite, and calcite. Most of the zones show prograde alteration with depth, with high temperature minerals either overprinting or occurring as later precipitation.

Furthermore, hydrothermal alteration was used to establish zones based on the first appearance of index minerals which are temperature dependent. The minerals include zeolites, quartz, chlorite, epidote and actinolite. From the analysis, five alteration zones were established. The results are presented in figure 4 and are as follows: the unaltered, zeolites-smectite, chlorite, epidote-chlorite, and actinolite-epidote zones. Detailed description of the zones is as follows:

Unaltered zone (0-154 m CT): This is the uppermost zone characterized by oxidation but no signs of hydrothermal activity. It is composed of fresh unconsolidated pyroclastics, rhyolite and rhyolitic tuff showing moderate to extensive degree of oxidation in fractures and vesicles.

Zeolites-smectite zone (154-560 m CT): The occurrence of low temperature alteration minerals zeolites and fine-grained clays marks the entry into this zone. The first appearance of zeolites (thomsonite) is observed at 176 m CT but only in one sample analysed. Progressive alteration is evident with chalcedony and quartz appearing at 190 m and 416 m CT respectively implying thermal temperatures >180℃. Both minerals are persistent in this zone together with oxides, pyrite, and minor calcite. This is also evident in veins and vesicles with fine-grained

clays and zeolites deposited at first at shallower depths but after that chalcedony, quartz and minor calcite deeper in the well.

Chlorite zone (560-1000 m CT): The zone is marked by the appearance of high temperature clays at 560 m CT in vesicles in association with secondary quartz and the disappearance of chalcedony. Chlorite is also observed as a replacement product of feldspars and mafic minerals. Mineral zonation of quartz >> chlorite is evident at 572 m CT further showing increase in temperatures to >230℃. Other mineral phases observed in this zone include; oxides, sphene, calcite, hematite, and minor platy calcite at 784-822 m CT, which may be an indication of boiling.

Epidote-chlorite zone (1000-1656 m CT): The upper limit of this zone is marked by the first appearance of epidote at 1000 m CT and indicates temperatures >240℃ in the geothermal system. Epidote occurs sporadically as a replacement product of feldspars and mafic minerals and/or direct void precipitation in this zone while alteration to chlorite is moderate to high. Epidote is observed to be overprinting calcite at 1868 m CT and 1884 m CT showing increasing alteration temperatures. Secondary quartz, hematite, oxides, calcite, platy calcite and pyrite are also observed in this zone.

Actinolite-epidote (1656-3136 m CT): This is the largest zone extending to the well bottom and is marked by the appearance of actinolite at 1656 m CT as an alteration product of pyroxenes. Actinolite occurs sporadically in this zone while increased abundance of epidote is observed at 1690 m CT and appears to the bottom of the well. Alteration minerals observed in this zone include chlorite, hematite, sphene, prehnite, calcite, platy calcite, secondary quartz, and pyrite. The intensity of alteration in rock units at 2300 m CT decreases significantly as observed in reduced calcite, pyrite, and chlorite mineralization down the well as well as disappearance of hematite and sphene.

3.3 Scanning Electron Microscope (SEM) analysis

Sample 1 at 1356 m is a highly altered trachyte, felsic rich and slightly fractured with micro-veins infilled with dark green clays, and indistinct mafic minerals. The petrographic image of the sample, figure 5a also shows some micro-veins. The alteration minerals in the groundmass and in veins elemental mapping was determined on figure 5b and the results presented in figure 6.

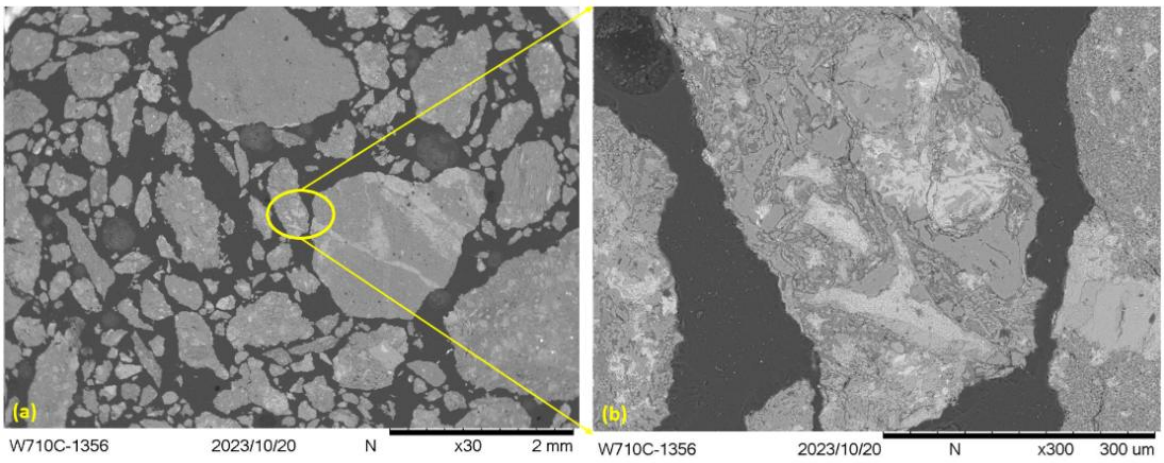


Figure 5: Backscatter Electron (BSE) image (a) with area of interest circled, and (b) is the magnified section

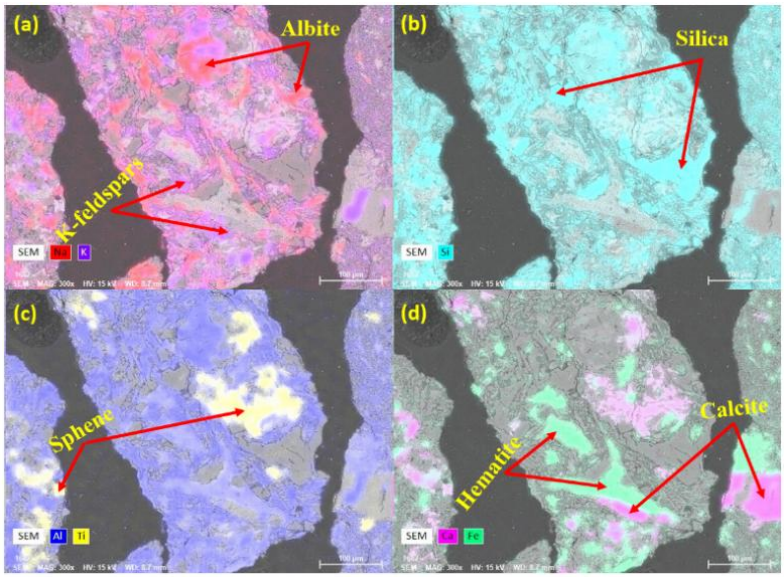


Figure 6: Elemental map of sample 1, 1356 m. The rock composition comprises of mainly Albite (Na), K-feldspars (K), Silica (Si) and Aluminium (Al) as shown in a, b, and c. Secondary minerals titanite (c), calcite (d) and hematite (d) occur in the rock matrix and in veins.

3.4 Permeability of well OW-710C

The existence and development of a geothermal resource requires heat, fluids, and permeability. Heat provides energy whilst the fluids act as a conveyor. Fractures can provide pathways for fluid flow both in the up-flow zones where there is sufficient heat and in the recharge zones which brings cooler fluids into the system (Hanano, 2000). As a result, adequate permeability is critical for targeting productive wells, but its nature is dependent on geology and in-situ stress conditions in the geothermal system (Perdana, and Mortensen, 2019).

In well OW-710C, two sources of permeability were identified during the analysis of rock cuttings. The presence of porous rocks and successive lithological units indicate a primary type whilst highly altered rock units, fractured intrusion margins and fault breccia show a secondary type of permeability. Fractured intrusion margins are generated during emplacement of magma, producing thermal stress that fractures the country rock. On the other hand, the fault breccia is associated with tectonism and is responsible for continuous rejuvenation of faults and fracture networks in the geothermal system. Precipitation of hydrothermal minerals in fractures and vesicles may, however, reduce permeability in a well or a system (Lawless, J., 2008). Consequently, directional drilling is done in Olkaria geothermal field targeting zones of enhanced permeability especially at faults/fracture intersections.

Location of permeable zones, commonly referred to as feed zones, were characterized using geological observations, drilling parameters and reservoir measurements as summarized in table 2. Fractures and possible fault zones exhibited intense fracture density, high alteration, and oxidation intensity. Moreover, increased pyrite, secondary quartz, calcite, and platy calcite mineralization in the rock cuttings is observed in these zones. Additionally, thin lenses of tuffs located at lithological contacts provided zones of horizontal permeability. While drilling, it was inferred that zones with high rates of penetration and loss of circulation might be permeable, however, caution should be exercised when interpreting significant losses encountered at depth due to introduction of aerated drilling technique.

The feed zones, as identified by the analysis of rock cuttings, were categorized as small, medium, and large depending on the extent of alteration, fracture density and areas with loss of circulation and is represented in figure 7. A total of four smaller feed zones were intercepted with majority located at depth. These zones ranged from depths of 1348-1374, 1974-2006, 2546-2572, 2718-2772 m CT. Additionally, ten medium-sized feed zones are proposed throughout the well. The depths of these feed points are 26-56, 58-90, 650-664, 1076-1094, 1162-1194, 1238-1248, 2130-2152, 2214-2268, and 2282-2372, 3046-3068 m CT. Finally, two large feed points were observed in the upper zone, between 116-128 m, and 822-940 m CT where it was cased off and. The permeable zones were mainly associated with highly fractured and altered rock units with minor to massive loss of circulation.

Pressure and temperature logs done after completion of drilling and recovery shows that the well has a maximum temperature of 256℃ at 1200 m CT but below that depth the temperature gradually lowers to ~215℃ at depth. Water rest level is located at 500 m while the pressure pivot point of the well is at 2300 m with 135 bars deduced to be the main aquifer controlling the system as shown in figure 7. Feed zones revealed in the well during pressure-temperature logs are noted in 509 m, 712 m, 952 m, 1066 m, 1243 m, 1370 m, 2129 m, 2345 m, 2547 m, 2737 m, and 3053 m CT.

The geological observations correlate with the above measurements in most cases; however, some feed zones represent the past/fossil permeability of the well which has probably been sealed by subsequent mineralization in the fractures over time. This is evident with the zones exhibiting high alteration intensities and fracturing but no observable evidence during drilling through loss of circulation nor in temperature logs carried out later. These feed zones include, 1460-1468, 1784-1792, 1870-1884, 1918-1956, 2020-2058, and 2092-2122 m CT. Table 2 gives a summary of both fossil and current permeable zones.

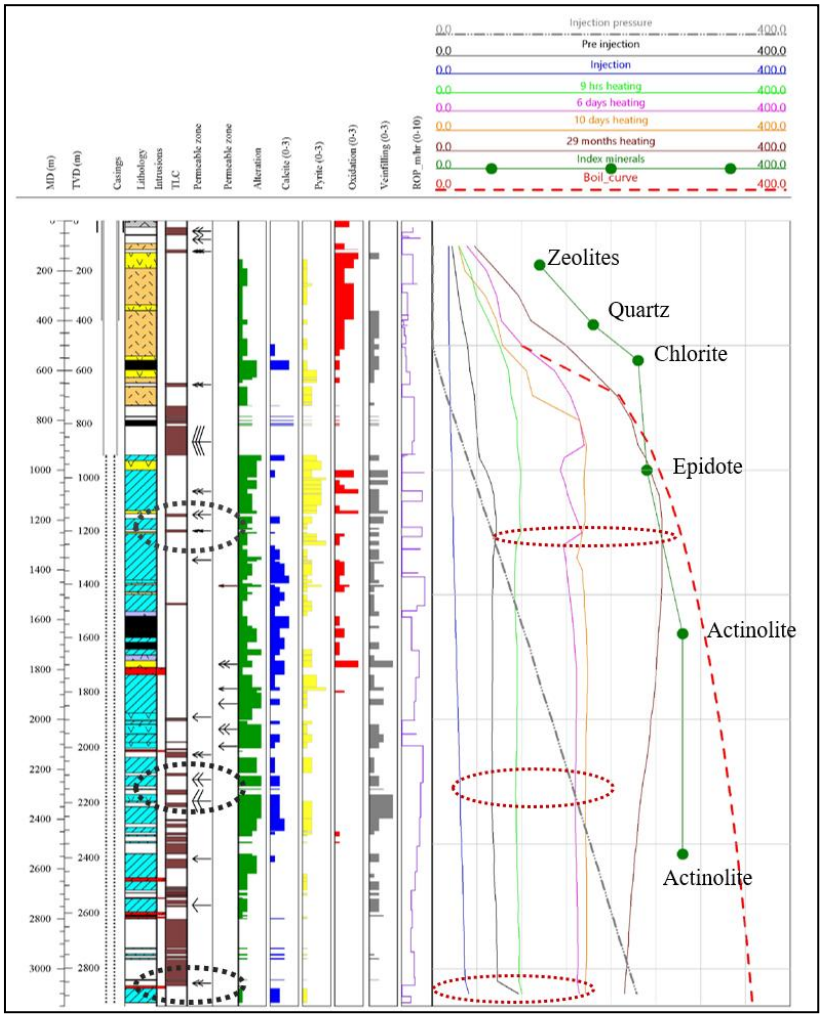


Figure 7: Lithology, permeable zones and temperature profiles and the comparison of alteration minerals, formation temperature and boiling point curve of well OW-710C.

Table 1: Summary of current and older/fossil permeable zones encountered in well OW-710C

Depth (m CT)	Category	Rock unit	Geological observation and reservoir measurements evidence
26-56	Medium	TLC	Loss of circulation, lithological contact
58-90	Medium	TLC	Loss of circulation
116-128	Large	TLC	Loss of circulation, lithological contact in highly fractured and porous rock units with high oxidation
650-664	Medium	TLC	Loss of circulation, underly slightly fractured rock

822-940	Large	TLC	Circulation loss, contact with highly altered and fractured rock; high calcite, secondary quartz & platy calcite precipitation; sharp temperature increase
1076-1094	Medium	Trachyte	Fractured rock; highly oxidized; pyrite mineralization; high rate of penetration
1162-1194	Medium	Breccia, TLC	Fractured, brecciated, and porous rock, loss of circulation, secondary quartz and pyrite mineralization; lithological contact
1238-1248	Medium	TLC	Circulation loss, contact with fractured and porous rock; secondary quartz mineralization; high rate of penetration; small cooling point
1348-1374	Small	Trachyte	Highly altered and slightly fractured rock
1974-2006	Small	Trachytic tuff	Partial losses, lithological contact
2130-2152	Medium	TLC	Loss of circulation, lithological contact; fractured rock units
2214-2268	Medium	TLC, trachyte	Loss of circulation, highly altered and slightly fractured rock, high epidote mineralization with minor quartz and calcite
2282-2372	Medium	TLC, trachytic tuff, trachyte	Loss of circulation, highly altered and fractured rock, high epidote mineralization with minor quartz
2546-2572	Small	Trachyte	Partial losses, slightly fractured, high oxidation
2718-2772	Small	Trachyte	Lithological contact, partial losses, slightly fractured rock
3046-3068	Medium	TLC	Lithological contact, underly slightly fractured rock, sharp temperature increase
Historical/paleo permeable zones in the well			
1460-1468	Sealed	Trachyte	Highly altered and moderately fractured rock, lithological contact, moderately high rate of penetration
1764-1792	Sealed	Breccia	Highly fractured and brecciated zone, high oxidation, lithological contact, calcite and quartz precipitation
1870-1884	sealed	Trachyte	Highly altered and moderately fractured rock, pyrite mineralization, lithological contact
1918-1956	Sealed	Trachyte	Highly altered and fractured rock; epidote mineralization
2020-2058	Sealed	Trachytic tuff	Lithological contact, highly altered and slightly fractured rock
2092-2122	Sealed	Trachytic tuff	Lithological contact; partial losses; highly altered and slightly fractured unit

3.5 Temperature conditions of well OW-710C

3.5.1 Thermal history

The study of thermal history gives a glimpse of the past and current reservoir conditions of an area. This understanding can be used to predict changes in a geothermal system with continued utilization. Comparison of the first occurrence of hydrothermal temperature dependent minerals and current formation temperatures in the system gives an impression of the thermal changes in a reservoir, whether the area around the well is in equilibrium, cooling or heating up (Helgadóttir, et.al. 2010). For well OW-710C, the heat up profile after twenty-nine months was used as the formation temperature although a downflow is observed where the temperature drops gradually from ~256℃ at 1200 m CT to ~215℃ at 3100 m CT. There is a very slow heat up in this well one below the casing shoe and another at depth which may be attributed to interception of the Ololbutot fault which is believed to bring cooler fluids into the geothermal system (Okoo, 2013, Kandie, 2017, Katana, 2019). However, the other two wells, OW-710A, and OW-710B, drilled in the same well pad but in different trajectories show temperatures above 300℃ at depth with no reversal in downhole temperatures. A cross-section of the measured temperatures from well OW-39B to OW-727 as shown in figure 8 indicates the signs of cooling at depth in the study well.

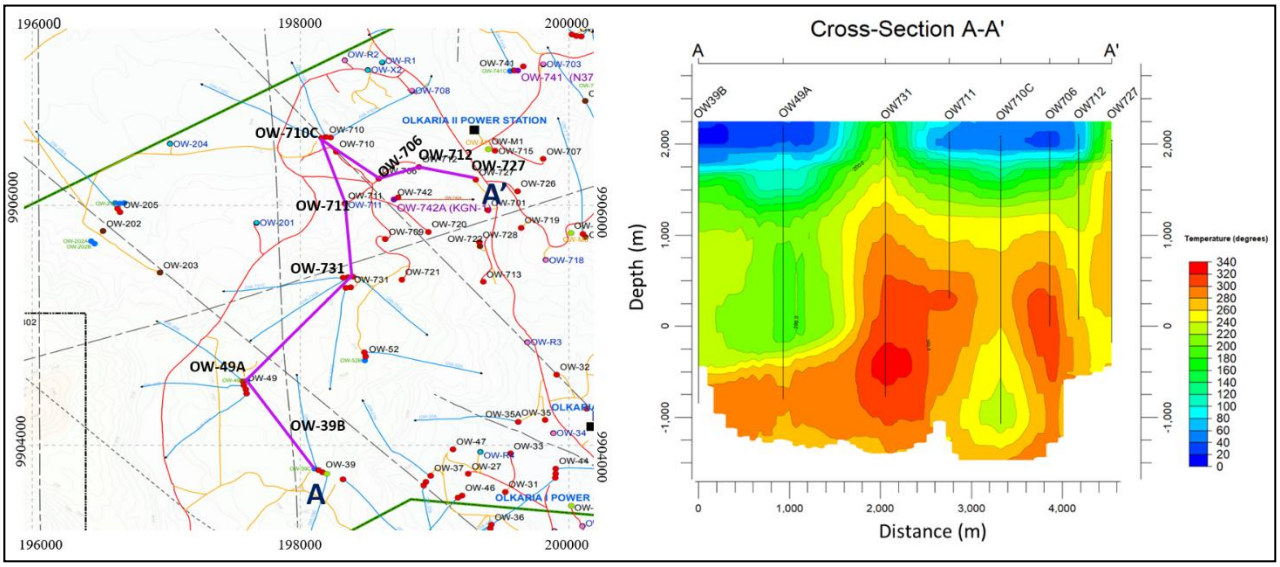


Figure 8: Location and cross-section of measured temperatures around well OW-710C from well OW39B to OW727 (A-A´)

The comparison of hydrothermal and the formation temperature in figure 7 reveals three zones in the well, the upper zone between 0-960 m CT where there appears to be cooling since the height of geothermal activity with the occurrence of alteration minerals having higher temperatures than the current conditions suggest. Secondly, between 960-1300 m CT, the system seems to be at equilibrium. Lastly, the zone below 1300 m CT, appears to have cooled down. Furthermore, the boiling point curve in the upper zone is slightly lower than the hydrothermal alteration indicating that past water table may have been higher than where it is currently.

4 DISCUSSION

Stratigraphic analysis revealed four main rock formations intercepted in this well. Namely, the upper Olkaria volcanics which are comprised of pyroclastics and rhyolites with minor intercalations of rhyolitic tuffs and basalt. Second, are the Olkaria basalts that forms an important zone capping the geothermal system. It is encountered between 740-822 m CT although the exact boundary could not be defined because of massive circulation losses encountered between 822-940 m CT. Underlying this zone are the plateau trachytes which are the main reservoir rock in Olkaria geothermal field. They occur persistently down the well bottom with interlayers of minor rhyolite, basalt, breccia, intermediate rock, tuffs (rhyolitic and trachytic) and intrusions. Intermediate rock is the rare unit observed in this well at 1586 m in contact with trachyte and basalt and at 1764 m CT between trachyte and magmatic intrusive breccia. Lastly are the minor intrusives which occur as thin layers < 30 m thick, cutting the plateau trachytes. The intrusions are important for transferring heat to shallower levels and at the same time may have enhanced vertical and/or horizontal permeability by breaking the country rock during their emplacement. This is evident at 1792 m CT, where brecciated zone was intercepted above a micro-granite that showed intense fracturing and extensive oxidation.

The occurrence and distribution of hydrothermal mineral assemblages was used to determine alteration zones, sequences of mineral deposition and areas with enhanced and restricted permeability. From the analysis, five distinct alteration zones were established by the first appearance of index minerals used as geothermometers. First is the unaltered zone, between 0-154 m CT characterized by interception of fresh rocks that are mainly oxidized with no evidence of hydrothermal alteration. The second zone is the smectite-zeolites zone, marked by occurrence of low temperature clays and zeolites. Evidence of prograde alteration from 40℃ to 180℃ is noted in this zone with appearance of chalcedony and quartz at 190 m CT and 416 m CT. Thirdly, chlorite zone occurs between 560-1000 m CT and characterized by first appearance of chlorite in vesicles and apparent disappearance of chalcedony. Mineral zonation at 572 m CT which shows chlorite overprinting secondary quartz further confirm increase in thermal temperatures from 180℃ to 230℃ in the well. Fourthly, is the epidote-chlorite zone between 1000-1656 m CT, evidenced by first appearance of epidote, a high temperature alteration mineral associated with entry into the reservoir in a high temperature geothermal system. Lastly, the actinolite epidote-zone, at depth marked appearance of actinolite at 1656 m CT. It indicates paleo thermal conditions >280℃.

Mineral sequences were characterized by precipitation of low temperature hydrothermal minerals in veins and vesicles at the shallower depth. These include oxides, zeolites, fine-grained clays, chalcedony, and secondary quartz. Apparently, no distinct zonation was observed in the zone but only gradual changes in type of minerals

occurring as infills. As you go deeper, intermediate alteration minerals, secondary quartz and chlorite begin to occur as amygdales. At depth, below 1800 m CT, infills is mainly by epidote with minor chlorite and secondary quartz. However, in some instances calcite appears to be overprinting epidote at 2042 m CT and 2068 m CT.

The use of scanning electron microscope showed accurate mineralogical and textural analysis which further enhanced understanding of the complex crystallization process and hydrothermal alteration mineralogy at a micro-scale. The tool can therefore be used to characterize sequence of mineral formation revealing the temperature formation trends of minerals and their reactions in a geothermal system.

Fractures and faults provide pathways for fluid flow in a geothermal system. Drilling of well OW-710C targeted the Ololbutot fault zone at depth in order to strike a permeable zone. The fault was intercepted at 1174 m CT shown by high brecciation and fracturing with extensive oxidation. This could have been an important feed zone in the well but apparently it may be responsible for gradual cooling of the well as observed in the temperature recovery. Fluid inclusion studies of well OW-39A by Okoo, 2013 about 3 km south of this well, imply that at one time in geothermal history, the fault acted as flow for hot fluids but has reversed probably by recent events to a cold geothermal barrier. This may be evident in well OW-710C with extensive oxidation and persistent occurrence of calcite at depth. Overall, three important zones were established to be areas of slightly enhanced permeability. These are, one aquifer just below the casing shoe and at the interception of the Ololbutot fault, two the zone at 2300 where pressure pivot point was established and at 3050 m CT where there is an apparent temperature increase. The paleo permeability of the well appears to have been good, however, the current observations shows that there is restricted permeability at depth probably due to the self-sealing effect of secondary minerals especially calcite.

Temperature recovery logs after 29 months shows gradual heat-up from surface to 1200 m CT where the maximum temperature of ~256℃ is recorded. Later, the well reveals down-flow trend to bottom hole temperature of ~214℃. There is apparent slow heating up in the well probably due to cooler fluids influx in the well or absence of a large hot feed zone at depth. The occurrence of calcite and platy calcite at depth and observations made in vesicles where calcite overprints epidote suggests cooling might have happened in the system or influx of low temperature fluids that necessitated precipitation of calcite, (Franzson, H., et al., 2008).

5 CONCLUSIONS

The following conclusions can be drawn based on the study of the well:

The main lithological rock units encountered in this well are pyroclastics, rhyolite, basalt, intermediate rock, trachyte, breccia, tuffs and intrusives.

Hydrothermal alteration gives a direct evidence of water-rock interaction, fluid pathways and chemical and physical conditions that existed during formation or precipitation of minerals.

Rock composition, permeability, fluid chemistry, temperature and pressure conditions and duration of fluid-rock interactions influence the occurrence and distribution of alteration minerals.

Five alteration zones were observed in the well based on the first appearance of index minerals. There are, unaltered zone, smectite-zeolites, chlorite, epidote-chlorite, and actinolite-epidote zones.

Mineral paragenesis showed a prograde deposition sequence with low temperature alteration minerals noted at shallower depth and at deeper depth high temperature alteration minerals are prevalent.

The permeability networks in well OW-710C is controlled by fractures and faults. Furthermore, interception of thin layers of tuffs especially in contact with other rocks showed evidence of horizontal permeability. The current conditions however reveal that the enhanced permeable zones that existed may have been sealed by secondary mineralogy because of persistence of calcite mineralization at depth.

The highest temperature recorded in the well is ~256℃ at 1200 m CT but gradually drops to ~215℃ at 3100 m CT. This may be attributed to influx of cooler fluids into the geothermal system.

Comparison of alteration and measured temperature shows slight cooling is present in the upper and lower zones of the well but at equilibrium between 960-1300 m CT.

The boiling curve appears below the alteration minerals indicating that the water table may previously have been higher than the current level.

The well appears to be at the boundary between the recharge zone and the upflow zone to the east with wells, drilled on the same pad, having bottom hole temperature >300°C.

REFERENCES

Browne, P.R.L., 1970: Hydrothermal alteration as an aid in investigating geothermal fields. Geothermics, 2, 564–570.

Browne, P.R.L., 1984: Lectures on geothermal geology and petrology. UNU-GTP, Iceland, report 2, 92 pp.

Chapman, G.R., Lippard, S.J., and Martyn, J.E., 1978, The stratigraphy and structure of the Kamasia range, Kenya rift valley. Journal of the Geological Society, 135, 265-281.

Chorowicz, J., 2005: The East African Rift System. J. African Earth Sciences, 43, 379-410.

Clarke, M.C.G., Woodhall, D.G., Allen, D., and Darling G., 1990: Geological, volcanological and hydrogeological controls on the occurrence of geothermal activity in the area surrounding Lake Naivasha, Kenya, with coloured 1:100 000 geological maps. Ministry of Energy, Nairobi, 138 pp.

Conti, P., Pistis, M., Bernardinetti, S., Barbagli, A., Zirulia A., Serri, L., Colonna, T., Guastaldi, E., and Ghiglieri, G., 2021: Tectonic setting of the Kenya rift in the Nakuru area, based on geophysical prospecting. Geosciences 2021, 11 (2), 80 pp. https://doi.org/10.3390/geosciences11020080.

Gebrehiwot Mesfin, K., 2010: Subsurface geology, hydrothermal alteration and geothermal model of northern Skardsmyrarfjall, Hellisheidi geothermal field. University of Iceland, MSc thesis, UNU-GTP, report 5, 65 pp.

Earth Science Australia, 2021: Energy and minerals, website: http://earthsci.org/index.html

Franzson, H., 2008: Chemical transport in geothermal systems in Iceland: Evidence from hydrothermal alteration. Journal of Volcanology and Geothermal Research, 173, 217-229.

Hanano, M., 2000: Two different roles of fractures in geothermal development. Proceedings of the World Geothermal Congress 2000, Kyushu - Tohoku, Japan, 2597-2602.

Helgadóttir, H.M., Snaebjörnsdóttir, S.A., Níelsson, S., Gunnarsdóttir, S.H., Matthíasdóttir, T., Hardarson, B.S., Einarsson, G.E., and Franzson, H., 2010: Geology and hydrothermal alteration in the reservoir of the Hellisheidi high temperature system, SW-Iceland. Proceedings of the World Geothermal Congress 2010, Bali, Indonesia, 10 pp.

Kandie, R.J., 2017: Borehole geology and thermal history of Well OW-737, Olkaria geothermal field, Kenya. Report 14 in: Geothermal Training in Iceland 2017. UNU-GTP, Iceland, 187-220.

Katana, C.N, 2019: Borehole geology and alteration mineralogy of well OW-205, Olkaria geothermal field, Kenya. Report 15 in: Geothermal Training in Iceland 2019. UNU-GTP, Iceland, 261-295.

Koilege, T. and Warui, D., 2018: Structural influence of the Gorge farm fault to hydrothermal alteration, mineral paragenesis in the Olkaria Northeast field; Case study of OW736A, OW734 and OW732C. Proceedings of the 7th African Rift Geothermal Conference, Kigali, Rwanda, 11 pp.

Lawless, J., 2008: Introduction to geothermal geological principles – Module 3. Proceedings of the Western Pacific Regional Branch/ Indonesian Geothermal Association INAPA seminar, Bali.

Munyiri S. K., 2016: Structural mapping of Olkaria Domes Geothermal Field using geochemical soil gas surveys, remote sensing and GIS. Master's thesis, Faculty of Earth Sciences, University of Iceland, Iceland, 108 pp.

Okoo, J., Omiti, A., Kimunya K., and Saitet, D., 2017: Updated conceptual model of Olkaria geothermal field Naivasha, Kenya. Geothermal Resources Council Transactions, 41, 18 pp.

Okoo, J.A., 2013: Borehole geology and hydrothermal mineralisation of well OW–39A, Olkaria East geothermal field, Naivasha, Kenya. Report 24 in: Geothermal Training in Iceland 2013. UNU-GTP, Iceland, 547-574.

Omenda, P.A., 1998: The geology and structural controls of the Olkaria geothermal system, Kenya. Geothermics, 27-1, 55-74.

Omenda, P.A., 1994: The geological structure of the Olkaria west geothermal field, Kenya. Proceedings of the 19th Stanford Geothermal Reservoir Engineering Workshop, Stanford, CA, 125-130.

Otieno, V., Okoo, J., Munyiri., S., Wanjohi, D., and Wanjohi A., 2014: Structural mapping of Olkaria Southwest field, Olkaria geothermal project. Kenya Electricity Generating Company, Kenya, internal report, 41 pp.

Perdana, T.S.P., and Mortensen A.K., 2019: Characterizing the subsurface structures and determination of in-situ stress orientations using Acoustic Borehole Images: A case study from Theistareykir geothermal field, Northeastern Iceland. GRC Transactions, 43, 735-753.

Strecker, M.R., Blisniuk, P.M., and Eisbacher, G.H., 1990: Rotation of extension direction in the Central Kenyan Rift. Geology, 18, 299.

Shanks III, W.C.P., 2012: Hydrothermal alteration in volcanogenic massive sulfide occurrence model. U.S Geological survey, Reston - Virginia, 2010-5070-C, 16 pp.

Wohletz, Kenneth, and Grant Heiken. Volcanology and Geothermal Energy. Berkeley: University of California Press, 1992.